Paper No. 166

ISMS 2016

Analysis of failure in a salt room and pillar mine

Farid Laouafa, Mehdi Ghoreychi

Institut National de l'Environnement Industriel et des Risques- INERIS, F-60550 Verneuil-en-Halate, France

ABSTRACT
Failure mechanisms have been investigated in a salt mine (Alsace Potash mines, Esat of France) excavated by the room and pillar method, a part of which is under study for chemical waste storage. This part is located at a depth of about 550 meters. Some singular failure modes appear in the roof mine. These modes are perpendicular to the axis of the gallery and are created by tensile stresses. Such a failure mode is rarely observed in classical mines (coal, construction stones, etc.). 3D modelling of the site has been required for accurate description of the physical mechanisms. The results show that the failures and more generally the roof behaviour are controlled by the deformation of the pillars inducing tensile forces in the roof. The results also show that the creep or the viscoplastic behaviour of the salt is a key element that explains the existence of such failure and their evolution over time. A parametric analysis of the properties of overburden, geometrical pillar features slenderness, confirm the conclusion. Namely, time-dependent deformation of large salt pillars generates their lateral extension and induces roof deformation and failure in tension. The numerical results are in full agreement with in-situ observations.
KEYWORDS: Salt mine; modelling; failure; creep

1. INTRODUCTION

Part of the salt mine belonging to Alsace Potassium Mines (MDPA) excavated by the room-and-pillar method has been used as a storage area for industrial waste (Figure 1).



Figure 1: Example of waste storage.

Storage began in 1999, in a specifically designed area (rooms and pillars) with a configuration comprising galleries 2.8 to 3 m high and 5.5 m wide, with pillars 20 m wide per side. Convergence measurements were taken at regular intervals and observations were also recorded regarding the mechanical behaviour of the structures. The storage project was stopped in 2002 and several options are being considered regarding the future of the site.

Cracks in the mine roof and bed separations were observed. In particular, transverse cracks relative to the axis of a gallery appeared in 2015 in addition to longitudinal cracks of the roof and bed separations. In order to determine the mechanical strength of the mine, INERIS was asked by the MDPA to identify the origin and consequences of these cracks.

The present study focuses in particular on the network of cracks due to mechanical failure (caused by the stress levels) observed in the roof and facings of some galleries running perpendicular to their axis. These more or less open cracks intersect a longitudinal fracture. The aim of this article is to analyse the mechanisms that led to this mode of failure in the roof.

Numerical modelling shows that the origin of the “transverse” cracks perpendicular to the axis of the galleries is linked to the creep of the salt pillars. In other words, the mechanism of deformation of the roof in the immediate vicinity is controlled mainly by that of the pillars. As these pillars are extremely massive (20 m wide), during their vertical and transverse deformation (continuous deformations related to salt creep), they pull down the roof in the immediate vicinity.

Although fracturing phenomenon along the axis galleries is often encountered in underground mines and quarries (coal, building stone...), transverse cracking is much more rare. Indeed it is strongly related to the intrinsic nature of salt, which deforms as there are stress deviators within it. It is on this mechanism that the paper will focus.

*Corresponding author – email: farid.laouafa@ineris.fr

2. DESCRIPTION OF THE SITE

The site examined by this study covers an area of about 4 hectares, 700 m x 600 m. It is located at a depth of approximately 550 m and exploited by the classical abandoned room and pillar method. The pillars are 20 m x 20 m square. The chambers are 5.5 m wide and 2.8 m high (Figures 2 and 3). The worked proportion (ratio of excavated surface to total surface) is 38%. Storage is accessible through aisles called double tracks, 4m wide, separated by 3m-wide pillars.



Figure 2: Section through Storage Area and location of cracks (blue) (MDPA, 2015) (Key: Bloc – Block).

Figure 3 is a zoomed-in image showing the design of the access tracks.

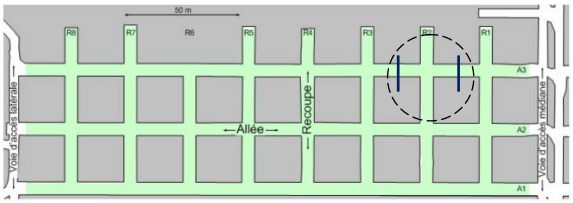


Figure 3: Zoomed-in image of pillars, aisles and intersections and location of cracks (blue) (MDPA, 2015). Key : Voie d'accès latérale - Side access route; Voie d'accès médiane - Middle access route; allées - aisles; recoupe - intersection; R1, R2... - I1, I2...

The site is located in the Alsace Potassium Mines which have been exploited throughout the last century. The formerly exploited level is about twenty meters above the level of storage. A very large pillar called *stot* was left for the overlying exploitation.

This is an unworked part, and includes two Potash layers worked by the method of making long cuts before caving in the roof (by removing the support structure).

Thus, significant subsidence of a maximum of 5.5 m was measured at the surface. The storage area is more or less affected by mechanical disturbances, induced caving, and *stot*.

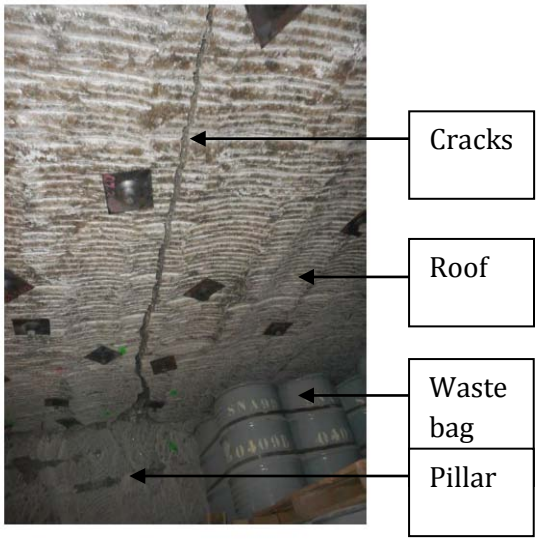


Figure 4: View of a transverse crack in the roof (*MDPA 2015*).

A visual inspection of the site revealed the existence of Mode 1 open cracks (Figure 4). One of the vertical cracks runs longitudinally in the direction of the track, practically in the middle of it (classic "flexion" mechanisms) resulting in horizontal traction.

It is however intersected by cracks perpendicular (transversal) to the track (Figure 4). These cracks are mainly at mid-width of the (20 m wide) pillars. It was observed that the transverse cracks are more or less open. They cross the roof and facings of the track.



Figure 5: Example of separation of roof (source, *MDPA 2015*).

As for bed separation (Figure 5), this affects the bed of rock salt in the roof immediately above the

tracks at the marly-anhydrite insoluble interlayers that are frequent at MDPA site.

In order to analyse the mechanical response of this structure, we must correctly define the intrinsic characteristics of its constituent material, namely salt, which will be the subject of the next section.

3. MECHANICAL BEHAVIOUR OF SALT

The main aspects of the rheological behaviour of rock salt are generally the same, whatever the variety. They can be summarised as follows:

1- a more or less marked aptitude for creep.

2- the absence of any viscoplasticity.

3- the rates of deferred deformations increase, in a non-linear manner, with deviatoric stress.

4- the rate of creep also increases exponentially with temperature. This dependency is expressed by the Arrhenius Law.

5- salt creep is accelerated after a crack occurs (resulting in so-called called "tertiary" creep observed in the laboratory, which results in the sample being ruined).

6- salt creep is accelerated in the presence of humidity and brine.

7- Above a certain level of stress, salt will crack. Unlike creep, the damage threshold of salt depends both on the mean stress and the deviator (like most rocks).

8- the damage thresholds (microcracking) and macroscopic breaking (maximum resistance) thresholds of salt fall in the presence of brine.

In light of these main traits of the thermomechanical behaviour of rock salt, two main rheological models have been proposed for the viscoplastic behaviour (creep) of this material: i) The Lemaitre model. According to this model, salt creep slows down over time and its development is expressed by a time power law, ii) the Norton (also called Norton-Hoff) model, widely used for salt throughout the world. This model considers that beyond a short transient phase, creep reaches a stationary state (linear evolution). We would also point out that the Norton and Lemaitre models are designed for the viscoplastic behaviour of rock salt and are not aimed at modelling the damage and rupture of this material. We used in this study the Norton model, on the basis of our findings on the results obtained during a previous study (Laouafa, 2010) focussing on the *in situ* convergence measurements (Figure 6).

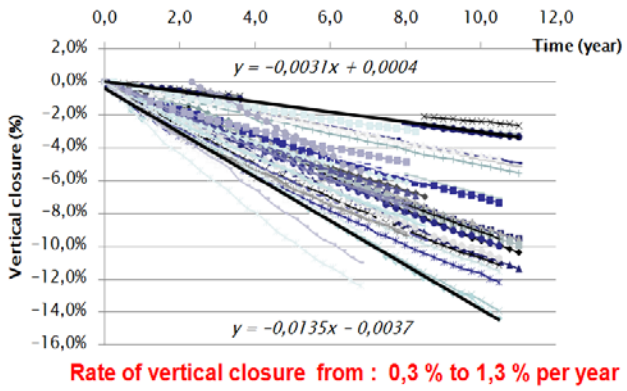


Figure 6: Rate of vertical closure, at different points of the mine (*MDPA 2015*).

Figure 6 clearly shows the linearity of convergence as a function of time, hence the use of the Norton model described below. For this model, the rate of viscoplastic strain $\dot{\underline{\underline{\varepsilon}}}^{vp}$ is expressed as follows (in tensor form):

$$\dot{\underline{\underline{\varepsilon}}}^{vp} = A\exp(-B/T)(Q/Q_0)^n \frac{\partial Q}{\partial \underline{\underline{\sigma}}} \qquad (1)$$

Q is the von Mises effective stress (MPa) and A, B, n : model parameters ; Q_0 = 1 MPa

Table 1: Creep model used by INERIS, adjusted against in situ measurements (Laouafa, 2010).

Elastic Parameters		Viscoplastic Parameters (Norton model)		
E (MPa)	ν(-)	A (j^{-1})	B(K)	n(-)
25000	0.25	0.022	4700	4.0

4. NUMERICAL MODELLING

4.1 Numerical Model and Assumptions

Although the storage area has no particular symmetry (Figure 3), a quasi-periodic "unit cell" can be seen, consisting spatially of pillars, aisles and intersections.

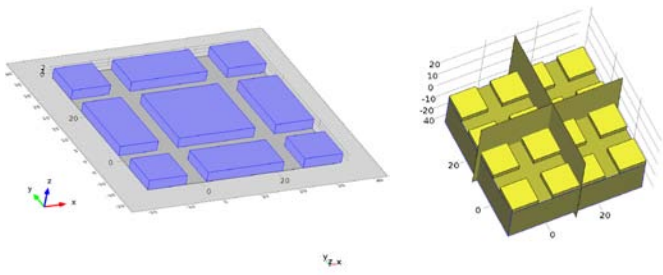


Figure 7: Plan and 3D view of the pillars, galleries and planes of symmetry.

In order to optimise the calculations without reducing their accuracy, a unit cell (Figures 7 and 8) composed of a 20 m x 20 m pillar 2.80 m high, aisles and intersections 5.5 m wide and the roof of the storage area positioned at -550 m (depth) was used.

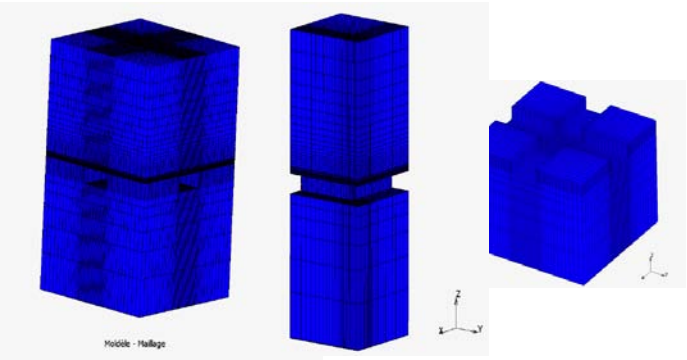


Figure 8: 3D view of pillar, galleries and unit cell and zoom-in view of the galleries.
Key: Modèle… - Mesh Model

The idealized geological medium is composed entirely of salt (Table 1), without taking into account the few marly seams in the roof. The dimensions of the model, the state of initial stress and the set boundary conditions are described below.

The dimensions of the model (Figure 8) are as follows:

- Width 25.5 m
- Length 25.5 m
- Height 42.80 m (wall 20 m and roof 20 m and pillar 2.80 m)

The boundary conditions are as follows:

- Plane of symmetry for the four vertical sides
- Plane of symmetry at the base of the model
- Pressure of 11.45 MPa (weight of the overburden).

The initial conditions are as follows:

- Range of initial lithostatic and isotropic stresses (hypothesis supported for evaporites):

$$\sigma_{xx}(z) = \sigma_{yy}(z) = \sigma_{zz}(z) = \gamma \times z \qquad (2)$$

In regards to the chronology and time span of the study, aisles and intersections were simulated numerically in about ten days. It does not follow the real chronology but allowed the stabilization of the evolving problem over time. The period of time considered since the voids were created is from 10 to 15 years.

4.2 Numerical results

This sub-section is dedicated to numerical results. We will focus only on the tensile stresses generated in the gallery roof, the main subject of this paper. Figure 9 shows the spatial extent of the zones under horizontal traction (Syy, stress component) (blue) affecting the roof and pillars after 10 years of creep. Note that Syy (orthogonal to the gallery axis) tractions develop on facets perpendicular to the axis of the gallery. Note also that the edge of the pillars and part of the roof is also affected by tractions.

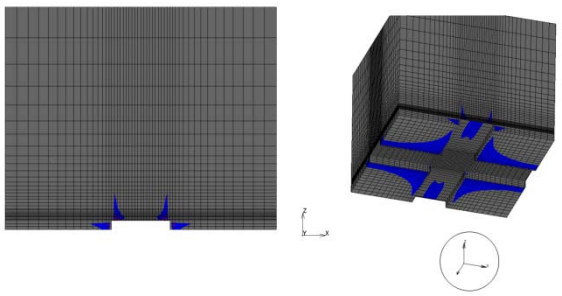


Figure 9: Positive horizontal Syy Stress (traction): Side view (left) and bottom view of the roof 10 years after excavation (obtained using the reference model).

Figure 10 shows (wireframe view) the 3D spatial distribution of the zones subjected to Syy traction .

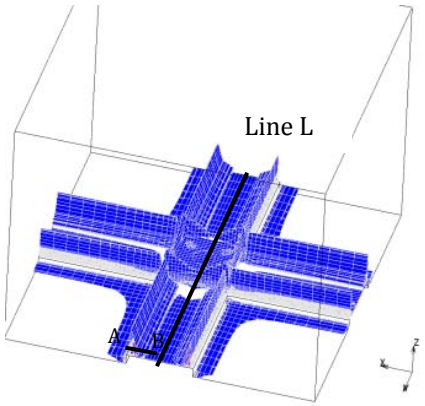


Figure 10: 3D view of the zones affected only by traction in direction y (Syy > 0) in the roof and pillar after 15 years (obtained using the reference model). The aisle, intersection, roof and pillars are shown.

From a more quantitative viewpoint, the paper is interested in what follows the time evolution of these tractions induced by creep of the pillars. For this Line L (parallel to the gallery axis), in direction y, located at mid-span of the roof, and segment AB,

located along the edge of the model (Figure 11) (perpendicular to the gallery) is considered.

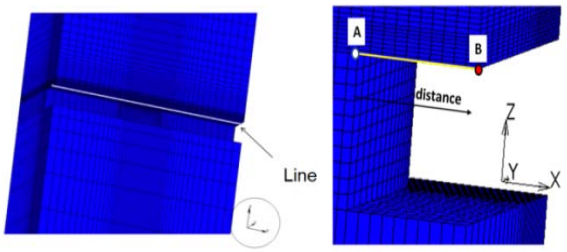


Figure 11: Definition of Line L under analysis passing through the roof of the storage area and parallel to the y-axis and Transverse segment AB (perpendicular to the axis of an aisle), located on the roof at mid-width of the pillar.

Figure 12 shows the distribution of horizontal stress Syy along Line L at two moments: 5 and 10 years. Initially (all structures in virgin state), Syy equals around -13 MPa (negative due to compression).

The redistribution of the stresses due to the works (here modelled with no phasing and virtually instantaneous) at t=0 changes continually over time. Note, for example, that 5 years after the works, Syy stress is still under compression but gradually comes under traction domain.

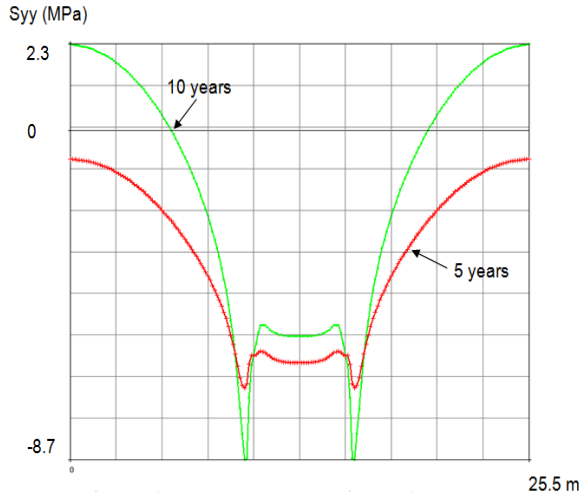


Figure 12: Distribution of horizontal stress Syy along line **L** at 5 and 10 years (computed using the reference model). The horizontal-axis represents the distance in m and the vertical-axis the stress in MPa. The sign convention is that of continuum mechanics (stress positive in traction and negative in compression).

This result is confirmed in Figures 13 and 14, which focus solely on the time evolution of the horizontal stress Syy at point B and for different configurations (hard or soft roof, slenderness, or excess-load roof).

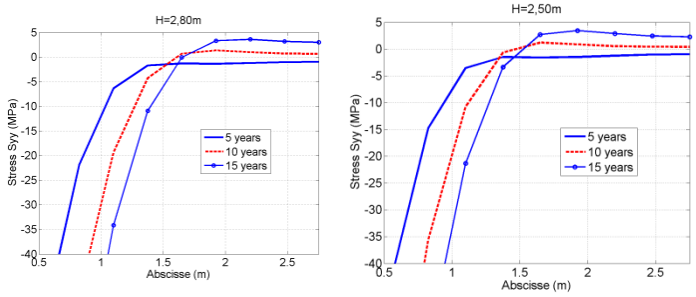


Figure 13: Distribution of Syy stress along segment AB (Figure 10) after 5, 10 and 15 years. For two pillar heights (H).

Key: - Abscisse - distance-axis

A reduction in Syy stress was observed, passing gradually from compression to traction and reach failure state within 10 and 15 years. This corresponds exactly to the period when the cracks appeared in the roof.

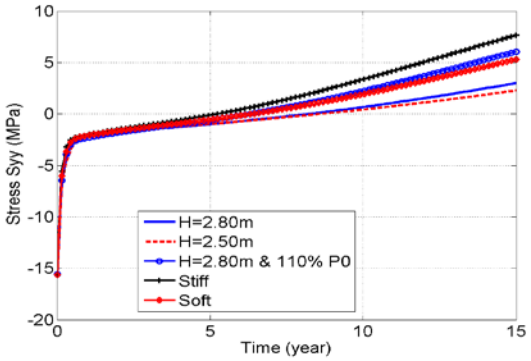


Figure 14: Temporal evolution of horizontal Syy stress at point B, as a function of time, since excavations began and for the different configurations.

These results show that the creep of the salt pillars is the main factor responsible for these significant variations in stress in the immediate roof area of gallery. The combined effect of this mode of failure and cracking occurred in two perpendicular directions (longitudinal and related roof separation) threatens the security of the site.

5. CONCLUSION

The 3D models (finite elements) clearly show that the creep of the salt mine is the primary cause of the cracking observed in situ. In particular, the transverse cracking affecting the galleries is caused by the gradual horizontal expansion of the pillars whose height continuously decreases (and leads to the expansion of the pillar, salt creep occurring with no variation in volume) due to the effect of salt creep. This expansion of the pillars forces the roof to stretch, which causes horizontal tensile stresses increasing over time. These stresses, on exceeding the salt's tensile strength (very low, 1 to 2 MPa maximum, in the short term and practically negligible in the long term) give rise to transverse cracks, which manifest themselves sooner or later in the pillars of all of the tracks.

6. ACKNOWLEDGEMENT

The authors wish to warmly thank the MDPA (Mines de Potasse d'Alasce) for their support and their active contribution to the work which allowed carry out the study.

7. REFERENCES

Cristescu N., Hunsche U. 1991. A constitutive equation for salt, 7th Int. Cong. Rock Mech., Aachen, Sept. 16-20, Balkema

Cristescu N., Hunsche U. (1998). Time effects in Rock Mechanics, Wiley.

Ghoreychi M. (1990). Conséquences du comportement thermomécanique du sel pour la conception et la sûreté d'un enfouissement de déchets radioactifs. Stockage en Souterrain, Presses des Ponts et Chaussées, 229-243.

Laouafa, F. (2010). Etude géomécanique du stockage de StocaMine. Rapport INERIS–DRS10-108130-14273A.

Laouafa, F. (2010). Analyse critique des études géomécaniques du stockage de StocaMine, Rapport d'étude INERIS-DRS-10-108130-04240A, 2 avril.

Mogenier, C. (2015). Rapport d'étude géophysique -Wittelsheim Bloc 21 / Allée 3 – 00029074. SOLDATA Geophysic.

Roman, J. (2015). Stockage de déchets StocaMine. Note de synthèse suite à la « visite d'inspection du 6 novembre 2014 ». MDPA.